POROUS HOT AIR TEA DE-ENZYMING AND CARDING MACHINE UNDER GAS–SOLID COUPLING CONDITIONS: NUMERICAL SIMULATIONS AND PERFORMANCE TESTING
/
气固耦合条件下多孔热风式茶叶杀青理条机数值模拟与性能试验

Haijun BI[*1, 2)], Pengcheng JIA[1,2)], Kuan QIN[3,4)], Lei YU[5)], Chengmao CAO[3,4)], Dongsong XIA[3,4)], Xinliang GUO[1,2)], Yang LIU[3,4)], Bin CHEN[3,4)], Yuzhen BI[1,2)]

[1)] State Key Laboratory of Tea Plant Biology and Utilization, Anhui Agricultural University, Hefei, China
[2)] School of Tea and Food Science and Technology, Anhui Agricultural University, Hefei, China
[3)] School of Engineering, Anhui Agricultural University, Hefei, China
[4)] Anhui Intelligent Agricultural Machinery Equipment Engineering Laboratory, Hefei, China
[5)] Anji Yuanfeng Tea Machinery Co. Ltd, Huzhou, China
Corresponding author, Tel:+8613965131157; E-mail address: bihaijun@ahau.edu.cn
First author, Tel: +8613965131157; E-mail address: bihaijun@ahau.edu.cn
DOI: https://doi.org/10.35633/inmateh-71-26

Keywords: *tea processing, de-enzyming, carding machine, gas–solid coupling, gas–solid flow, numerical simulation, performance testing*

ABSTRACT
The gas–solid coupling of a porous hot-air tea de-enzyming and carding machine was studied by means of computational fluid dynamics and discrete element coupling. In the numerical model, the discrete phase of tea particles was simulated using Rocky-DEM software, while the gas phase was described by ANSYS Fluent software. A mathematical model of the movement characteristics of tea particles in air was established according to the principle of fluid mechanics, to carry out dynamic analysis of tea particles' movement process and derive how the motion of gas and tea particles is governed. Three sets of prototype tests were carried out on the basis of the design and simulation, and the average of their results taken. This showed that the hourly output of the test prototype was 3.89 kg/h, the bar-type rate was 89.14%, the de-enzyming moderation rate was 91.67%, and the average value of the measured effective operating temperature of the pot slot was 189 °C. The performance of the prototype was also tested and analyzed. After conducting a tea sensory evaluation expert appraisal, the sensory evaluation indices of the prototype-processed tea satisfied all current market requirements, being superior to those of the conventional de-enzyming and carding machine. The quality of the finished tea also met the agronomic standards and the operational requirements of the de-enzyming and carding machine.

摘要
通过计算流体动力学和离散元耦合的方法对多孔热风式茶叶杀青理条机的工作过程进行了气固耦合数值研究。在数值模型中，使用 Rocky-dem 软件模拟茶叶颗粒的离散相，ANSYS Fluent 软件描述气体相。通过研究并根据流体力学原理建立了茶叶颗粒在空气中运动特性的数学模型，以此来进行茶叶颗粒运动过程的动力学分析，分析气体和茶叶颗粒的运动规律。在设计与仿真的基础上，进行了三组样机试验，取 3 次试验结果的平均值，结果表明：试验样机的台时产量为 3.89 kg/h，成条率为 89.14%，杀青适度率为 91.67%，实测锅槽有效运行温度均值为 189°C；并在上述基础上对试验样机进行了性能测试与分析。经茶叶感官评审专家鉴定，加工后的茶叶感官评价指标均符合要求，各项指标均优于传统杀青理条机，制得的成品茶质量达到农艺标准，且满足杀青理条机的工作要求。

INTRODUCTION
Green tea is the main type of tea cultivated in China, ranked first in China's tea category, and it is the most common tea consumed by Chinese people (*You et al., 2023*). Both de-enzyming and carding play a vital role in tea processing; whether their joint effect is satisfactory or not directly impinges upon the appearance and quality of tea leaves (*Wang et al., 2022*).

De-enzyming refers to the use of an external high temperature to transfer heat to fresh tea leaves, to eliminate their oxidase activity. Doing so also vaporizes water, reducing the moisture content of parts of tea leaves, leaving them softer and easy to knead and shape, while also dispersing the smell of tea itself to produce a sweet aroma (*Cao et al., 2016*).

Carding is a method of processing tea leaves and turning them into strips, which facilitates subsequent processes, and it helps to promote the formation of desirable tea color, aroma, taste, and other qualities (*Yan et al., 2022*).

Currently, domestic and foreign researchers are mostly interested in the hot air roller de-enzyming process of the roller de-enzyming machine. Most of these studies compare the quality of de-enzyming leaves, by experience or by experiment, to investigate the most suitable parameters and equipment of tea de-enzyming process. For example, *Panchariya et al. (2002)* experimentally measured and studied the variation patterns of hot air temperature and air velocity with moisture content in the hot air-drying process of tea leaves. Later, with the help of Fluent software, *Xu et al. (2014)* revealed the heating condition during de-enzyming done by a leaf guide plate (segment design) when the angle of spiral rise is held constant. They verified whether the segmented design structure is effective at improving the de-enzyming quality. Employing an experimental approach, *Ye et al. (2014)* conducted a comparative study of the roller, steam heat, and steam heat-roller combination de-enzyming processes, assessing the sensory quality, tea composition, color, and aroma of the produced green tea.

Shi et al. (2015) used a coupled EDEM-Fluent technique to examine the effects of variation in roller speed, the number of leaf guides, the height of leaf guides, the width of leaf guides, and the structure of the hot air inlet on the de-enzyming quality during hot air de-enzyming process. Recently, *Yu et al. (2019)* applied Fluent-EDEM to the coupled simulation of an infrared de-enzyming machine and electric heating de-enzyming machine. They compared the temperature distribution of the flow field in the roller of two de-enzyming machines and the temperature distribution of flow field of tea particles after de-enzyming was completed. They concluded the de-enzyming efficiency, heat energy utilization, and de-enzyming effect of the infrared de-enzyming machine outperformed those of the electric heating de-enzyming machine. More recently, *Wang et al. (2022),* used CFD (Computational Fluid Dynamics) technology to simulate and analyze the temperature field of a trough-type de-enzyming and carding machine, aiming to solve the poor uniformity of temperature's distribution in the pot groove of the tea carding machine; their findings led to an idea to further improve the uniformity of temperature in the carding parts.

Porous hot air de-enzyming technology is a multi-component, multiphase thermal system composed of tea and hot air as its raw materials. In this paper, the 6CSL-800 tea de-enzyming and carding machine was selected as the research object. Tea was designated a discrete phase, while hot air was considered a continuous phase. Both discrete element software (Rocky-DEM) and fluid dynamics software (ANSYS Fluent) were used to carry out a joint simulation operation to analyze the coupling between the discrete field and flow field during de-enzyming and carding (*Li et al., 2021*). The operational process of the multihole hot air type tea de-enzyming and carding machine was studied, and this existing device prototype optimized and tested to achieve the goal of improving the tea de-enzyming quality and increasing the yield from leaves. However, relevant research based on the trough-type porous hot air de-enzyming technology is lacking, so further research work on that is necessary.

MATERIALS AND METHODS

General structure and working principle

As shown in Figure 1, the 6CSL-800 type tea de-enzyming and carding machine is mainly composed of a U-shaped multi-groove pot, a frame, an eccentric wheel, a crank slider mechanism, a hydraulic cylinder, a connecting rod, a motor, a fan, a gas heating device, a gas regulating valve, a gas conveying pipe, and other components (*Bi et al., 2022*). The over-all structure appears in Figure 1A. During its operation, the de-enzyming and carding machine delivers power to the U-shaped multi-groove pot via the belt drive and crank slider mechanism, realizing different changes in speed by altering the motor frequency to meet the needs of the tea processing process (Figure 1B).

The heating parts are distributed underneath the U-shaped multi-slot pot, which is driven by the crank slider mechanism for reciprocating linear motion.

The main technical parameters of the 6CSL-800 de-enzyming and carding machine presented in Table 1.

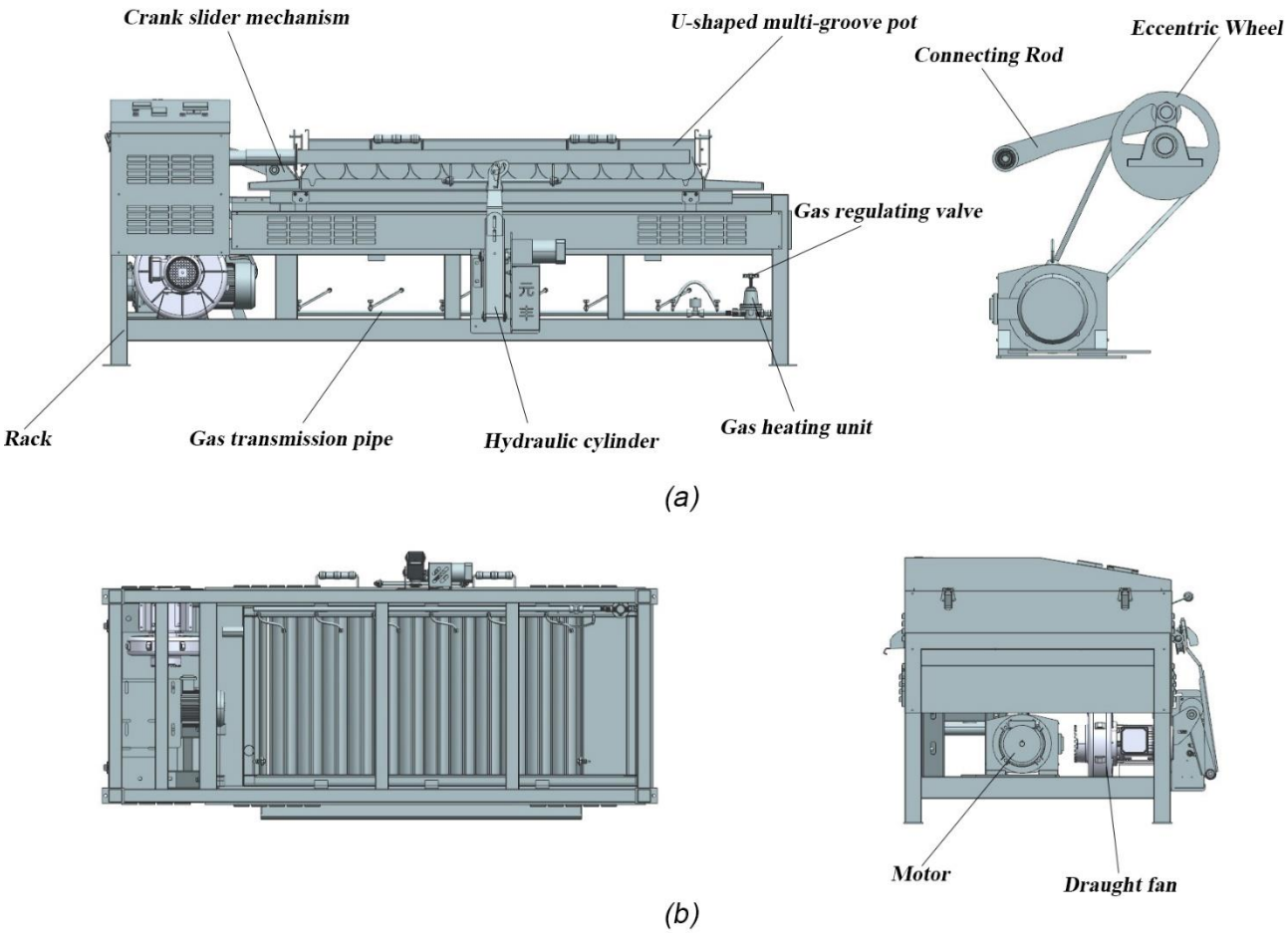

Fig. 1 - Schematic of the structure of the 6CSL-800 tea de-enzyming and carding machine
(a) Front view of the machine; (b) Upper and left view of the machine

Table 1

Main working parameters of the tea carding machine

Major parameter	Value
Boundary dimension (mm)	2450 × 1100 × 950
Pot groove size (mm)	1000 × 600
Rated power (kw)	0.55
Working voltage (V)	380
Output per hour (kg/h)	≥ 3.5

Key component design

The 6CSL-800 machine's key parts are its U-shaped multi-groove pot and crank slider mechanism. The former is an important component, in that the depth size of the U-shaped slot, the width size of the pot, the size of the angle between the inner wall of the pot and horizontal surface, and other factors directly affect the efficacy of the tea de-enzyming and carding. As Figure 2A shows, there are air holes on the left and right sides of the inner wall of the U-shaped multi-groove pot, and the hot air discharged from the holes could alone release and disperse the green odor of the tea leaves and thereby prevent the phenomenon of 'water boredom' (*Wu et al., 2022*). As depicted in Figure 2B, the connecting rod mechanism of the crank slider mechanism is the key component of the machine's transmission, by implementing the reciprocating motion of the U-shaped groove by linking to the U-shaped groove. In the process of movement, the connecting rod applies a forward thrust and a downward pressure to the U-shaped multi-groove pot. The servo motor then propels the driving wheel to rotate, whose rotation could drive the slave wheel, eccentric wheel, and connecting rod in turn to perform reciprocating linear motion. When the connecting rod carries out this reciprocating linear motion, it causes the fixed pushing plate and carding plate to swing back and forth, achieving the purpose of evenly carding the tea leaves.

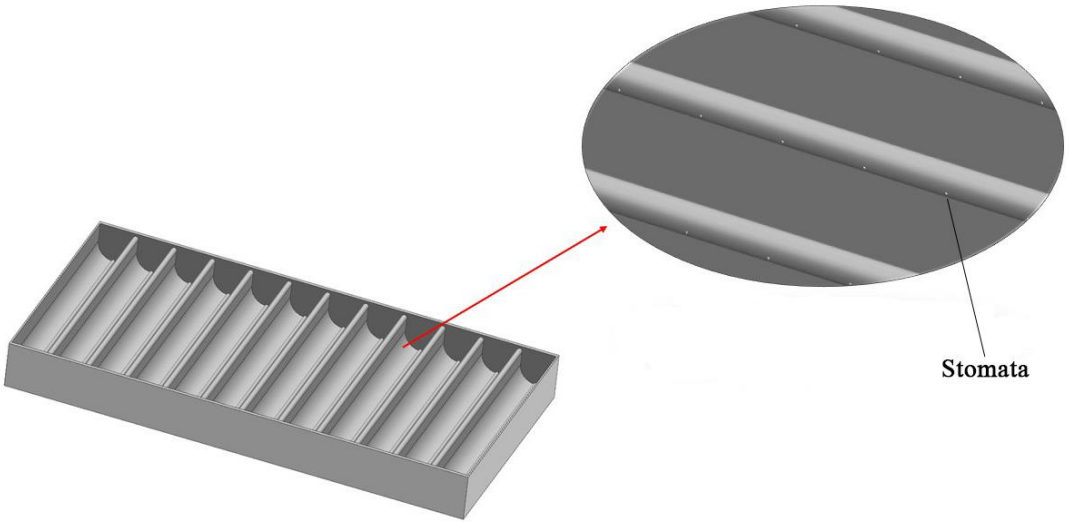

(a)

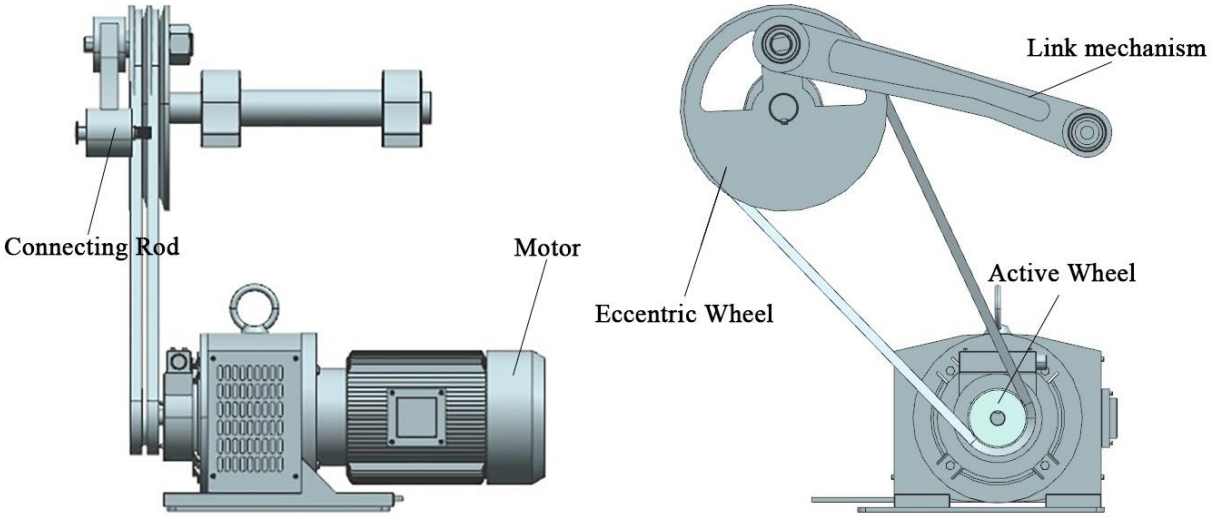

(b)

Fig. 2 - Structural diagrams of the key components

(a) Schematic diagram of the U-shaped multi-slot pot structure; (b) The crank slider mechanism

ANALYSIS OF THE MOVEMENT PROCESS OF TEA PARTICLES

The movement of tea particles in the pot groove is divided into three main stages. First, the tea particles move along the inner wall of the pot groove. Next, the tea particles leave the pot groove and undergo a throwing motion. Finally, the tea particles fall onto the pot groove' surface which entails collision movement. Ignoring the collision effect generated between tea particle and other particle, tea particle were treated as a single mass point, and a mathematical model of the motion characteristics of tea particle in air then established by following the principle of fluid dynamics; it was used to carry out a kinetic analysis of the motion process of tea particles (*Zhang et al., 2022)*.

Force analysis of the movement of tea particles along the inner wall of the pot groove

Here, a single tea particle was selected as the object of study, for which an absolute coordinate system was established on the ground and the motion process of tea particles along the inner wall of the pot trough was analyzed accordingly (*Wu et al., 2019*).

As illustrated in Figure 3, *AC* is the pot groove curve; point *B* is the location of the center of mass of the moving tea particle; *R* is the diameter of the tea particle, *n* is the normal vector of the mass point on the inner surface of the pot groove; *t* is the surface tangential vector of the mass point of the tea particle in the pot groove; and α is the angular acceleration.

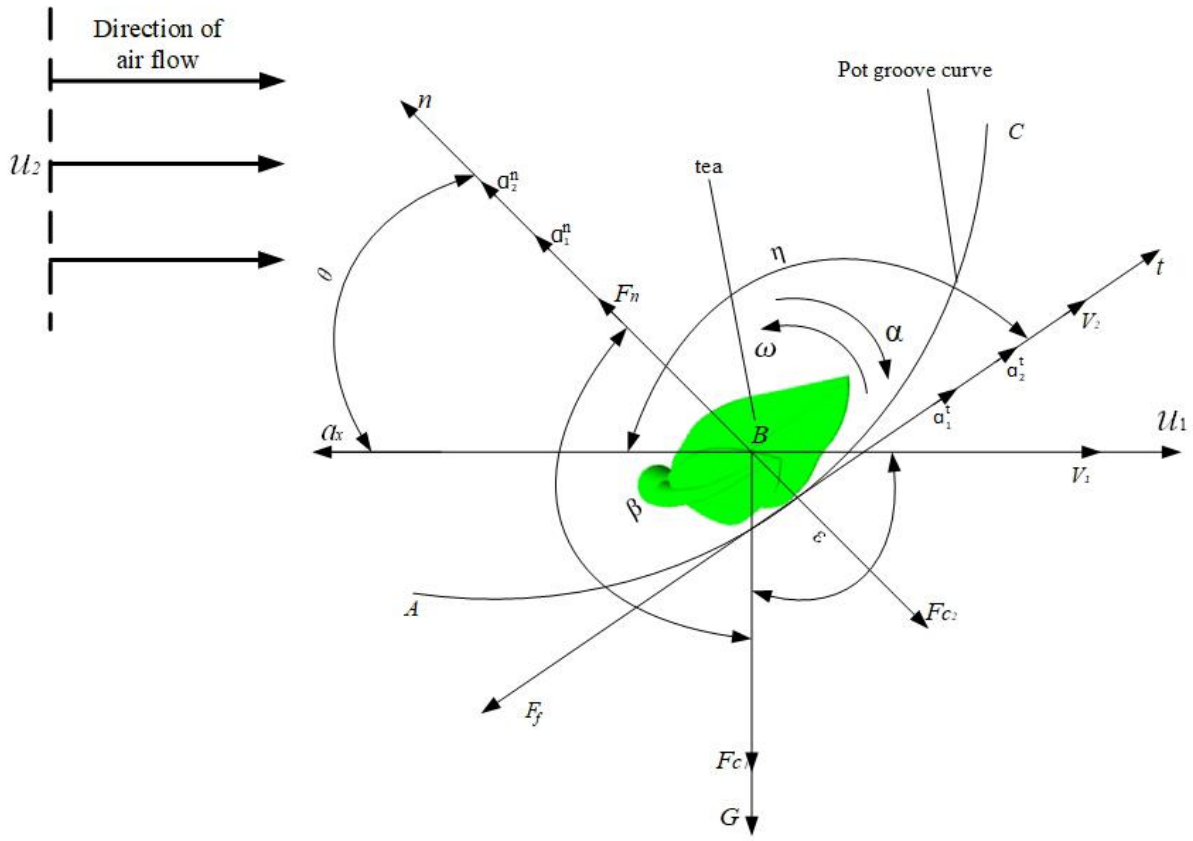

Fig. 3 - Force analysis diagram of tea particle tossing motion

As tea particles move along the inner wall of the pot trough under the action of the driving force, F_N<0, the relative average velocity of the friction force and tea particle's movement along the wall of the pot groove is in the opposite direction.

The Coriolis force acting on tea particles is as follows:

$$F_{c1} = -2m\omega \times V_1 = -2ma_{c1} \quad (1)$$

$$F_{c2} = -2m\omega \times V_2 = -2ma_{c2} \quad (2)$$

where:

ω is the angular velocity of tea particles (rad/s); V_1 is the velocity of reciprocating motion of the pot groove during operation (mm/s); V_2 is the relative velocity of the mass point when moving on the inner wall of the pot groove (mm/s); a_{c1} is the Koch acceleration of F_{c1} (mm/s²); and a_{c2} is the Koch acceleration of F_{c2}.

According to their force analysis, the support force of the pot groove wall surface on the tea particles when they are moving along the curve of the pot groove is obtained as follows:

$$F_N = -(G + F_{c1})\cos\beta + ma_2^n + F_{c2} \quad (3)$$

The friction force on the wall of the pot groove facing the tea particles is given by:

$$F_f = (G + F_{c1})\cos\varepsilon + ma_2^t = \mu F_N \quad (4)$$

where:

F_N is the support force of tea particles (in newtons, N) on the pot groove's wall; F_f is the dynamic friction between the mass point and inner wall of the pot groove (N); G is the gravitational force (N) acting on tea particles (m is the mass, g is the acceleration of gravity, fixed at 9.81 m/s²; $G = mg$); F_{c1} and F_{c2} is the Koch force generated by the mass point under the action of V_1 and V_2, respectively (N); β is the angle between the gravity G and the normal vector n (º); ε is the angle between the gravity G and the tangential vector t, (º); a_2^n and a_2^t are respectively the normal component and tangential vector of the absolute acceleration of the mass point in the direction of the pot groove's inner surface (mm); finally, μ is the friction coefficient of tea particles on the wall of the pot groove.

Analysis of the frictional and support forces affecting the tea particles leads to the following relationship between the tangential vector a_2^t and normal vector a_2^n of the absolute acceleration of tea particles on pot groove's inner wall:

$$ma_2^t = \mu[(G + F_{c1})\cos\beta - ma_2^n - F_{c2}] + (G + F_{c1})\cos\varepsilon \quad (5)$$

By analyzing the connection between vectors in Figure 2, the tangential vector a_x^t and normal vector a_x^n of tea particles' acceleration along the inner wall of the pot groove could be derived, as follows:

$$a_x^t = a_x \cos\eta \quad (6)$$

$$a_x^n = a_x \cos\theta \quad (7)$$

where: a_x is the acceleration of the pot groove under reciprocating motion (mm/s²); η is the angle between the acceleration of the pot groove's motion and the tangential vector t (º); and θ is the angle between the acceleration of the pot groove's motion and the normal vector n (º).

Given that the acceleration of tea leaves relative to the movement of the pot groove + acceleration of the inner wall of the pot groove = the absolute acceleration of tea particles, the latter could be obtained using a formula for point acceleration summation, as follows:

$$a_2^t = a_1^t + a_x^t \quad (8)$$

$$a_2^n = a_1^n + a_x^n \quad (9)$$

where: a_1^n and a_1^t are respectively the normal component and tangential vector of the mass point's acceleration in the direction of movement with respect to the inner surface of the pot groove (mm).

According to the force analysis diagram in Figure 3, the force acting on tea particles in the airflow when they move along the pot groove can be expressed this way:

$$u_1 = u_2 + V_1 - a_x \quad (10)$$

where: u_1 is the relative velocity of tea particles to the airflow (mm/s) and u_2 is the average velocity of the airflow (mm/s).

Force analysis of tea particles undergoing throwing and collision motion

A single tea particle was taken as the object of study, treating it as a mass point (*Zhang S. et al., 2020*). The absolute coordinate system is established on the ground, and the velocity direction of the tea particle and airflow is moving at an angle of θ with the horizontal direction, with no collision observed. The force analysis of the tea particle is presented in Figure 4.

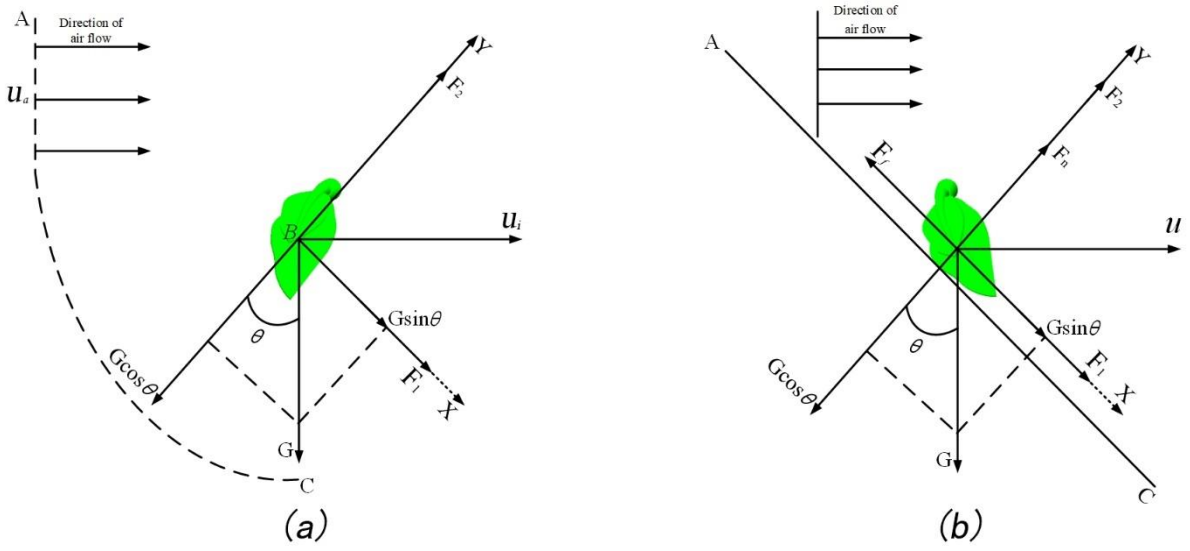

Fig. 4 - Force analysis diagrams of tea-particle throwing and collision motion

(a) Force analysis of the throwing motion of tea particles; (b) Force analysis of the collision motion of tea particles

As Figure 4 shows, *AC* is the pot groove curve, point *B* is the location of the moving tea particle's center of mass, and the left arrow points to the direction of airflow.

Assuming that the diameter of each tea particle is R, according to gas–solid two-phase flow theory, the force F_1 on the airflow from the equivalent tea particle diameter R_s is given as follows:

$$F_1 = k\ \rho\ S\ u_i^2 \tag{11}$$

According to Equation (11), it could be obtained as follows:

$$u_i = u_a - u_v \tag{12}$$

$$u_a = \frac{Q}{S_A} \tag{13}$$

where:

k is the resistance coefficient of a given tea particle; ρ is the density of air at room temperature under the machine's working conditions (kg/mm^3); S is the area of each tea particle facing the airflow (mm^2); u_i is the relative velocity of tea particles to airflow (mm/s); u_a is the average velocity of airflow (mm/s); u_v is the initial velocity of tea particles (mm/s); Q is the volume of airflow (mm^3/s); and S_A is the cross-sectional area of tea particle (mm^2).

According to the force analysis of tea particles, the following are obtained:

$$\begin{cases} F_x = F_2 - G\cos\theta \\ F_y = F_1 + G\sin\theta \\ G = mg \end{cases} \tag{14}$$

where:

F_x is the force acting on the tea particle along the vertical direction of motion (N); F_y is the force on the tea particles along the horizontal direction of motion (N); G denotes the force of gravity from the tea particles themselves (N); F_2 is the Magnus effect force (N); m is the mass of the tea particle, kg; and g is the acceleration of gravity of the tea particles (9.81 m/s^2).

The gravitational component force $G\cos\theta$ on the tea particles could be understood as the formation of differential pressure force with airflow vis-à-vis the Magnus effect force F_2 in reaching a phase equilibrium. The combined influence of various factors, such as airflow resistance F_1, and $G\sin\theta$, in the direction of motion of tea particles, could be derived using a set of differential equations for the motion of tea particle based on D'Alembert's principle, as follows:

$$\begin{cases} \dfrac{du_{vx}}{dt} = \dfrac{F_M}{m} - G\cos\theta \\ \dfrac{du_{vy}}{dt} = \dfrac{k\rho A\left(\dfrac{Q}{S_A} - u_v\right)^2}{m} + G\sin\theta \end{cases} \tag{15}$$

where:

u_{vx}, u_{vy} is the x, y direction of the tea particles speed, in mm/s.

Yet due to the constraints of certain factors, such as the angle between the groove wall and the pot groove's baffle, when the tea particles move they are bound to collide with the baffle. So, in addition to the above forces, they should also be subjected to the action of support force F_N and friction resistance F_f of the pot groove's inner wall. Applying D'Alembert's principle, the differential equations for the movement of tea particle is derived as follows:

$$\begin{cases} F_f = \mu F_N \\ \dfrac{du_{vx}}{dt} = \dfrac{F_M + F_N}{m} - G\cos\theta \\ \dfrac{du_{vy}}{dt} = \dfrac{k\rho A\left(\dfrac{Q}{S_A} - u_v\right)^2}{m} + G\sin\theta - \dfrac{\mu F_N}{m} \end{cases} \tag{16}$$

where: μ is the friction factor of the inner wall of the pot groove.

According to Equations (12-16), the acceleration of tea particles moving in the pot is influenced by the average velocity of airflow (u_a), the initial velocity (u_v) of tea particles, and the angle θ between the gravity of tea itself and the direction of the gravitational component of tea particles. Due to the action of airflow forces F_1 and F_2, the tea particles' acceleration when moving along the inner wall of the pot groove increases significantly, which causes them to bounce around when moving along the pot groove (*Luo, Cao, et al., 2022*). Because of the fixed diameter of tea particles (i.e., the cross-section area S_A of each tea particle is fixed), the average flow velocity u_a is greatly affected by the inlet flow rate, denoted by Q. Meanwhile, in the process of tea leaf carding, differences exist in the depth and width of different pot grooves, resulting in an inconsistency for the angle θ between tea particles and airflow velocity, which is influenced by not only the acceleration of tea leaves' own gravity in the vertical direction but also airflow disturbance. Moreover, the tea particles hit the inner wall of the pot groove, resulting in a smaller relative cross-sectional area of tea particles. Therefore, the average velocity of airflow u_a increases, which modifies the movement velocity of a given tea particle. The force analysis expounded above thus provides theoretical support for the subsequent simulation and experimental design (*Tang et al., 2021*).

DEM–FLUENT–BASED SIMULATION ANALYSIS

The Rocky-DEM's discrete elements, coupled with ANSYS Fluent's fluid dynamics software, were used here to simulate the operation process of a porous hot air type tea de-enzyming and carding machine (*Xue et al., 2022*). More specifically, the discrete element-based simulation software Rocky-DEM 2022 R1.2 was used to analyze the movement of tea particles in the pot groove, and ANSYS Fluent 2022 R1 was used to calculate the overall fluid dynamics of the model (*Geitani T. and Blais B., 2023*). The simulation parameters were set by Rocky-DEM software, with no adhesion presumed on the surface of tea particles. The Type C: Linear Spring Rolling Limit contact model was implemented for particle-to-particle interactions (*Tang et al., 2022*). The Hysteretic Linear Spring and Linear Spring Coulomb Limit contact force models were used for between the tea particles and walls of the pot groove, and the direction of gravitational acceleration was set. The basic parameters of tea particles and contact materials were set accordingly in the simulation test, whereas the contact parameters between tea particles and between them and the wall of the pot groove were set following the parameter-setting method proposed in literature (*Qin et al., 2022)*. These are listed in Table 2 *(Michiko et al., 2017)*.

Table 2

Basic parameter settings

Name	Parameter	Value
Tea particle	**Poisson's ratio**	0.38
	Density (kg·m^{-3})	562.4
	Shear modulus (Pa)	1×10^7
Pot groove	**Poisson's ratio**	0.3
	Density (kg·m^{-3})	7800
	Shear modulus (Pa)	7×10^7
Particle–particle	**Coefficient of restitution**	0.37
	Coefficient of static friction	0.5
	Coefficient of rolling friction	0.15
Particle–pot groove	**Coefficient of restitution**	0.4
	Coefficient of static friction	0.35
	Coefficient of rolling friction	0.1

Establishing the simulation model of tea particles

The Rocky-DEM software is able to render a real model of the particle shape on the basis of other 3D software. It can also use a custom polyhedron to import the particle model. Considering that the main purpose of the simulation process is to discern the movement track of tea particles in the pot groove and their full turnover in this groove, different shapes of tea particles could prolong the time required for the simulation's operation (*Wu et al., 2020*). Therefore, in practice, the axial length of tea particles should exceed their radial length of tea particles, so simplifying tea particles to spherical particles is inappropriate. Hence, in the present study, the tea particles were set as bar-type particles, with the bar-type tea particle model Straight Fiber built

on the basis of actual physical parameters of tea leaves (having a measured axial length of 24 mm and radial length of 2 mm). The ensuing shape of the tea particles after this modeling is shown in Figure 5.

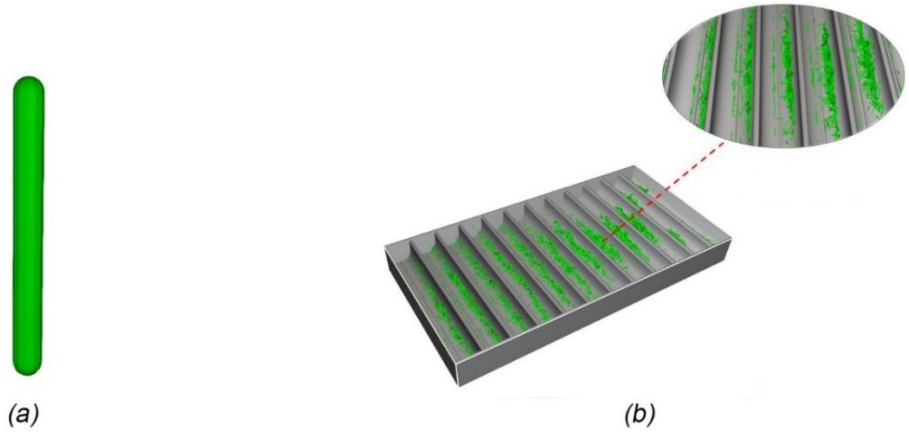

Fig. 5 - Tea particle simulation model

(a) Tea particle model; (b) Model of tea particles in the pot groove

Geometric model extraction and mesh generation in fluid domain

In this paper, using SolidWorks software, a 3D model of the whole structure of the porous hot air tea de-enzyming and carding machine was established. This model was appropriately simplified, by omitting those parts—such as the frame, gas appliances, and motor—not in direct contact with tea particles in the pot groove (*Luo et al., 2022*). Then, SolidWorks software was used to extract the fluid domain of the required simulation geometry model; the extracted fluid domain model was saved in an .iges format and imported separately into the ANSYS Fluent and Rocky-DEM software programs for the subsequent simulation operations (*Rakesh and Shibayan., 2023*), as illustrated in Figure 6. Structured meshing was presumed for the extracted fluid domain model; boundary conditions, such as INLET and OUTLET, were set; and the mesh was exported. The fluid domain mesh was imported to ANSYS Fluent software, the corresponding simulation parameters were set, and the k-epsilon (2 eqn) model was implemented for the turbulence model (*Xue et al., 2022*).

The working process of porous hot-air tea de-enzyming and carding machine was simulated by fluid dynamics. The air inlet connected to the fan at the bottom of the pot was set as the velocity inlet of the flow field, with the rate of air entering the fluid domain fixed (left unchanged). The airflow inlet was set to an 'Outflow' method, the inlet wind speed was set to 20 m/s (in accordance with the actual measured value), the inlet hot-air temperature was set to 350 K, the outlet pressure was set to 1 Pa, and the number of iterations was n = 1000. The specific simulation parameters are set out in Table 3. After all kinds of conditions and parameters were thus specified, the solving began (*Luo, Cao et al., 2022*).

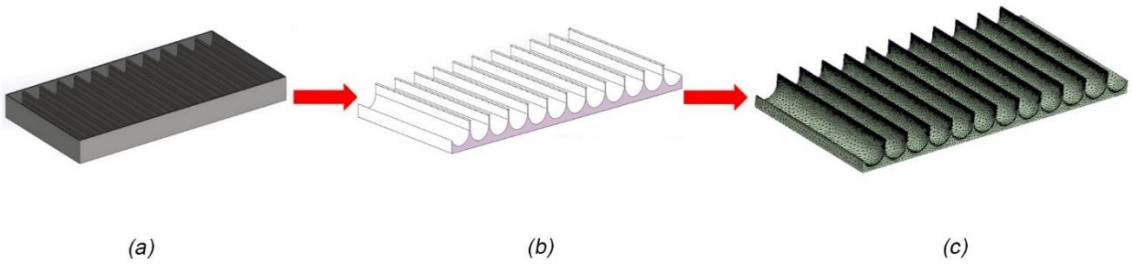

Fig. 6 - Fluid domain geometric model extraction and meshing

(a) Simplified model of pot groove; (b) The extracted fluid domain model; (c) Fluid domain meshing

Table 3

Fluent simulation parameter settings

PARAMETER	VALUE
Specific heat (K)	1006.43
Thermal conductivity (K)	0.0242
Velocity inlet (m/s)	20
Pressure outlet (Pa)	1
Backflow total temperature (K)	350
Number of iterations	1000

Coupling simulation process and result analysis

Coupling simulation process

After the solution for fluid motion was completed, it was post-processed by ANSYS Fluent software, to obtain the distribution nephogram and streamline diagrams of variable factors of the airflow field in the pot groove. As shown in Figures 7 and 8, the airflow was distributed into the pot groove via the inlet port on the bottom of the pot groove, and its velocity gradually decreased. After the airflow passed through a certain length, the airflow velocity gradually became stable. The airflow's speed at the airflow inlet of the pot groove was in a stage of deceleration, such that velocity of airflow in either section declined from the inside to the wall of the pot groove during deceleration. After airflow velocity is mostly stable, it is consistent on any section *(Qin et al., 2022*). When the airflow is in its deceleration stage, a pressure difference could appear on tea particles' surface, such that when they are propelled by airflow some of them could also be blown to pot groove's wall. When the tea particles are close to the wall of the pot groove, the airflow speed decreases, which leads to contact and even collision between the tea particles and wall.

As Figure 9 shows, after the post-processing of Fluent was completed, a Rocky workgroup was created in the ESSS module of the toolbox of ANSYS Workbench. After the coupling model was associated with the Rocky workgroup, 'Setup' was clicked to set relevant parameters. After doing so, the Setup of the Rocky workgroup was associated with the Solution of Fluent module, and then Setup was double-clicked to start Rocky for solving the coupling. Rocky-DEM and ANSYS Fluent were used for the coupling simulation analysis, and the movement trajectory of tea particles in the pot groove was then obtained, as depicted in Figure 10. When the tea particles move along the wall of the pot groove, they hit it many times, slowing their movement. Under the influence of airflow, the tea particles move at an accelerated speed, thus moving repeatedly until they complete the whole overturning process in the pot groove. Through the post-processing work of Rocky-DEM, the continuous distribution law of velocity and acting force between pot and tea particles in the differing motion stages under the condition of gas–solid coupling was obtained (Figure 11).

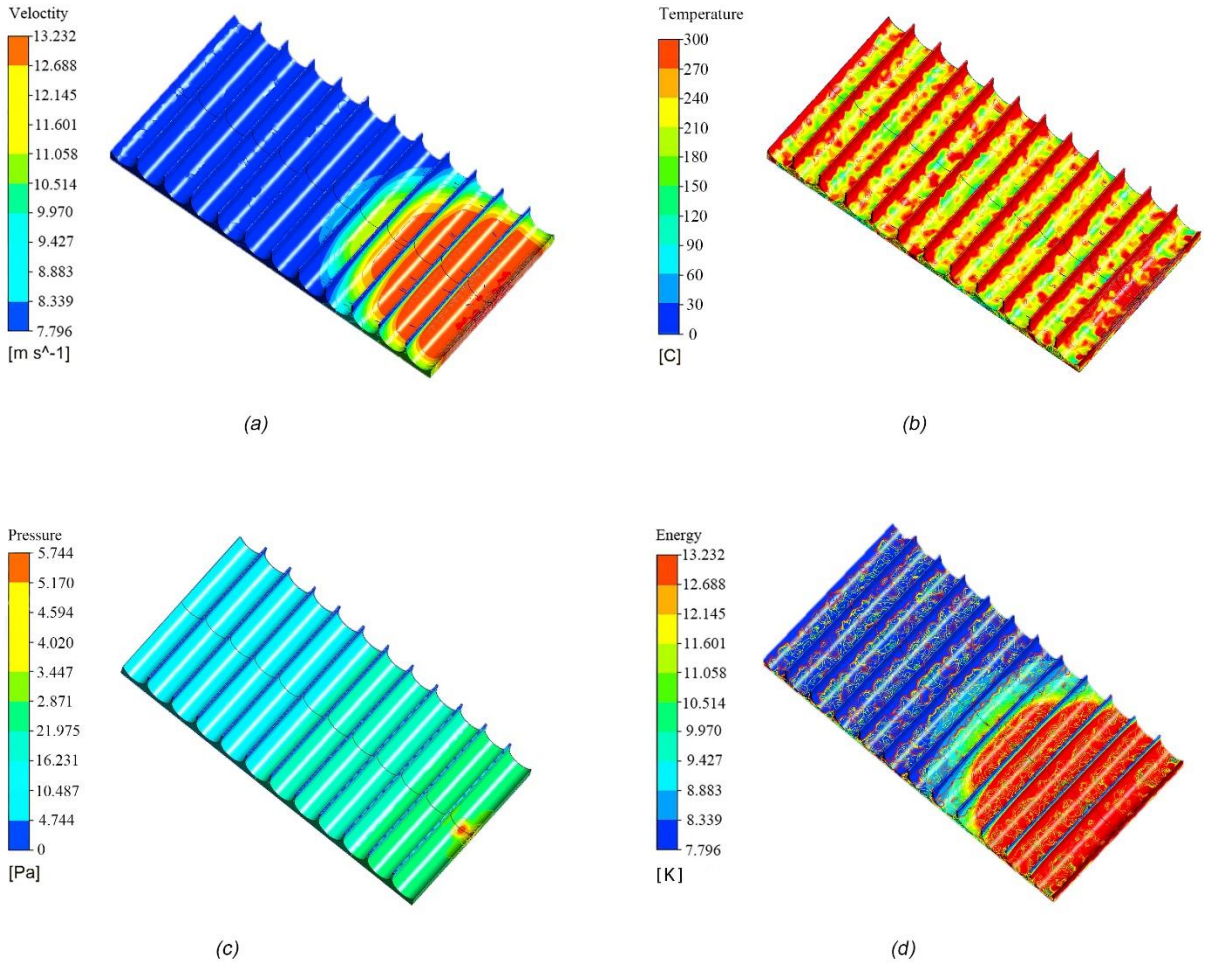

Fig. 7 - Fluid domain geometric model extraction and meshing

(a) Velocity cloud diagram; (b) Temperature cloud diagram; (c) Pressure cloud diagram; (d) Energy cloud diagram

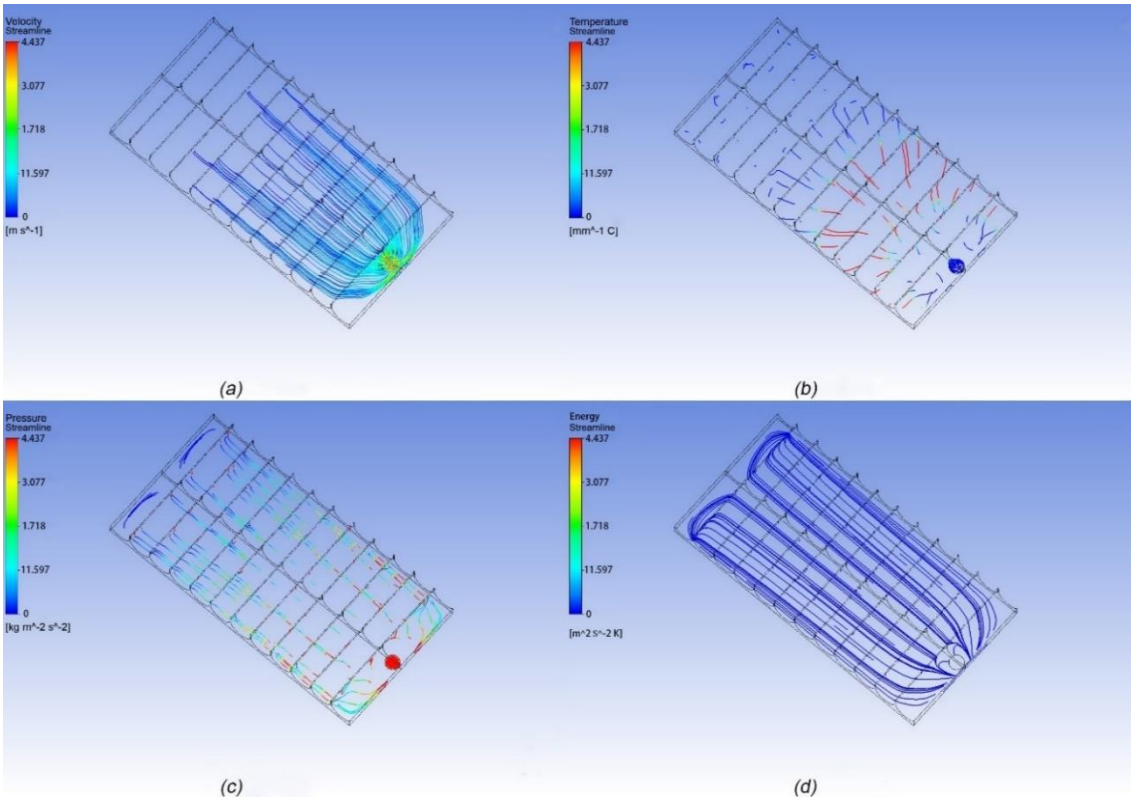

Fig. 8 - Streamline diagrams of the air flow field in the pot groove

(a) Velocity streamline diagram; (b) Temperature streamline diagram; (c) Pressure streamline diagram; *(d) Energy streamline diagram*

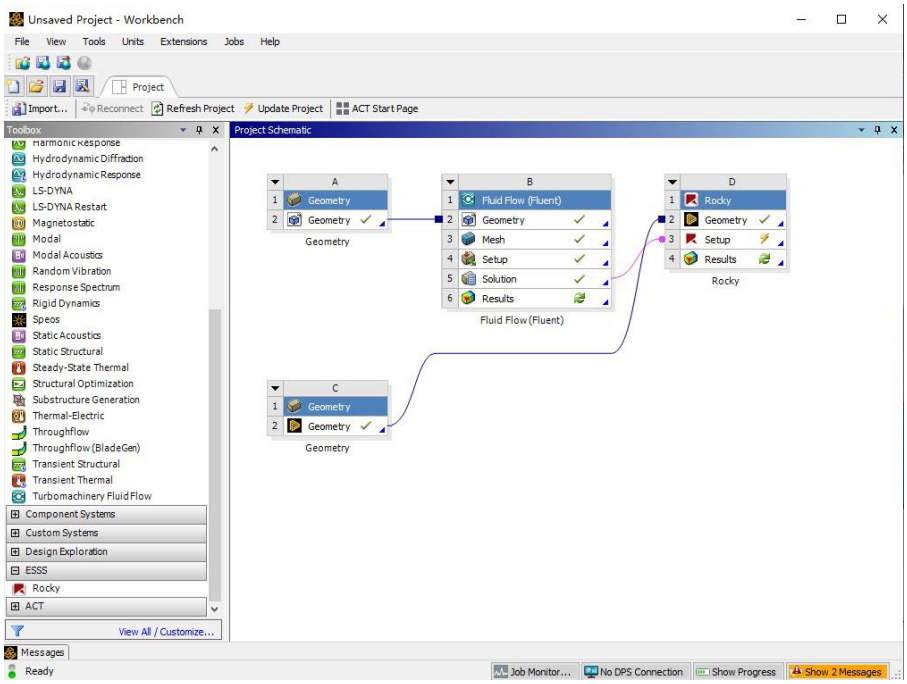

Fig. 9 - Co-simulation of Rocky-DEM and ANSYS Fluent

Simulation result analysis

In Rocky-DEM, the change condition of velocity, interaction force, and motion frequency between pot groove and tea particles under gas–solid coupling condition was analyzed using a block function (Figure 12). Under the same inlet wind speed, the movement speed and interaction force of tea particles gradually increase over time and then tended to stabilize. The force on the pot groove is mainly the interaction force generated by the collision with tea particles. Therefore, regardless of the influence of the interaction force between particles, its force is basically the same as the curve of the interaction force overtime generated by the tea particles' movement. As the pot groove moves in a reciprocating linear motion under the driving force of the motor, the motion frequency of the pot groove vis-à-vis the tea particles changes periodically. The pot groove,

however, is unaffected by any external torque; hence, its speed of reciprocating linear motion on the horizontal plane is a fixed value. When the inlet airflow velocity is constant, the movement speed of tea particles is basically the same at the same position in the groove.

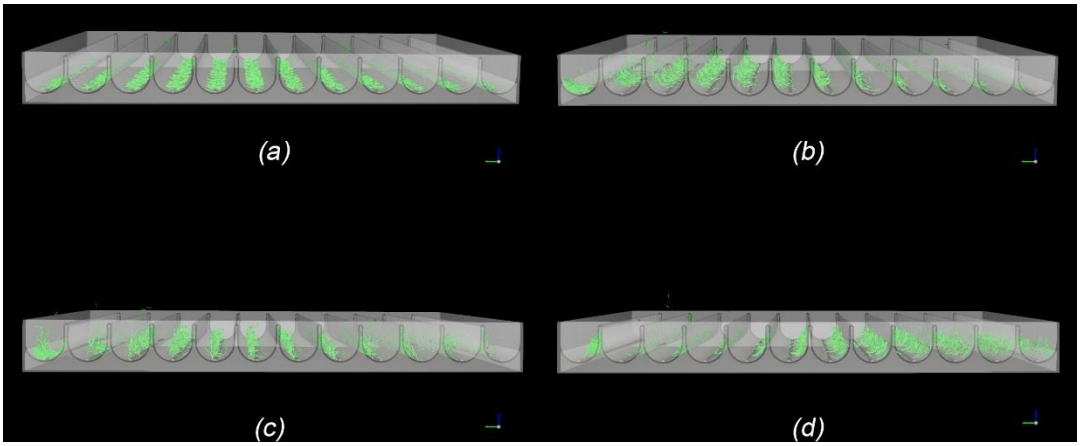

Fig. 10 - Movement trajectory of tea particles in the pot under the coupling condition

(a) The first stage; (b) The second stage; (c) The third stage; (d) The fourth stage

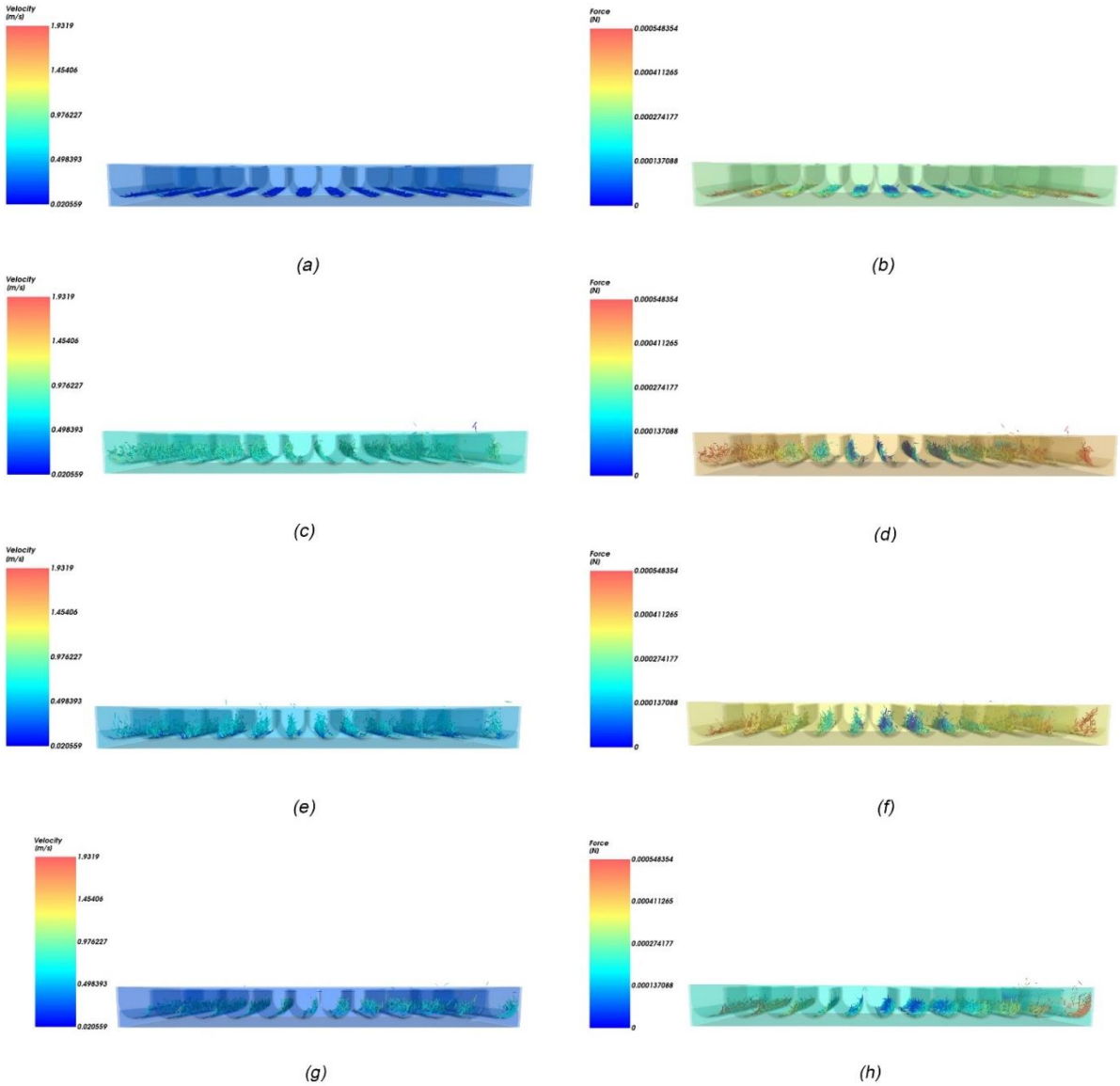

Fig. 11 - Continuous distribution of velocity and force in different stages of motion

(a) Continuous distribution of velocity in the first motion phase; (b) Continuous distribution of forces in the first motion phase; (c) Continuous distribution of velocity in the second motion phase; (d) Continuous distribution of forces in the second motion phase; (e) Continuous distribution of velocity in the third motion phase; (f) Continuous distribution of forces in the third motion phase; (g) Continuous distribution of velocity in the fourth motion phase; (h) Continuous distribution of forces in the fourth motion phase

Both Rocky-DEM and Fluent were used for the coupling simulation analysis. The distribution and motion state of tea particles in the pot groove were obtained, as were the changing curves for the speed, interaction force, and motion frequency of tea particles at differing positions of the groove under the same inlet airflow velocity. Collectively, these laid the foundation for the subsequent experimental design.

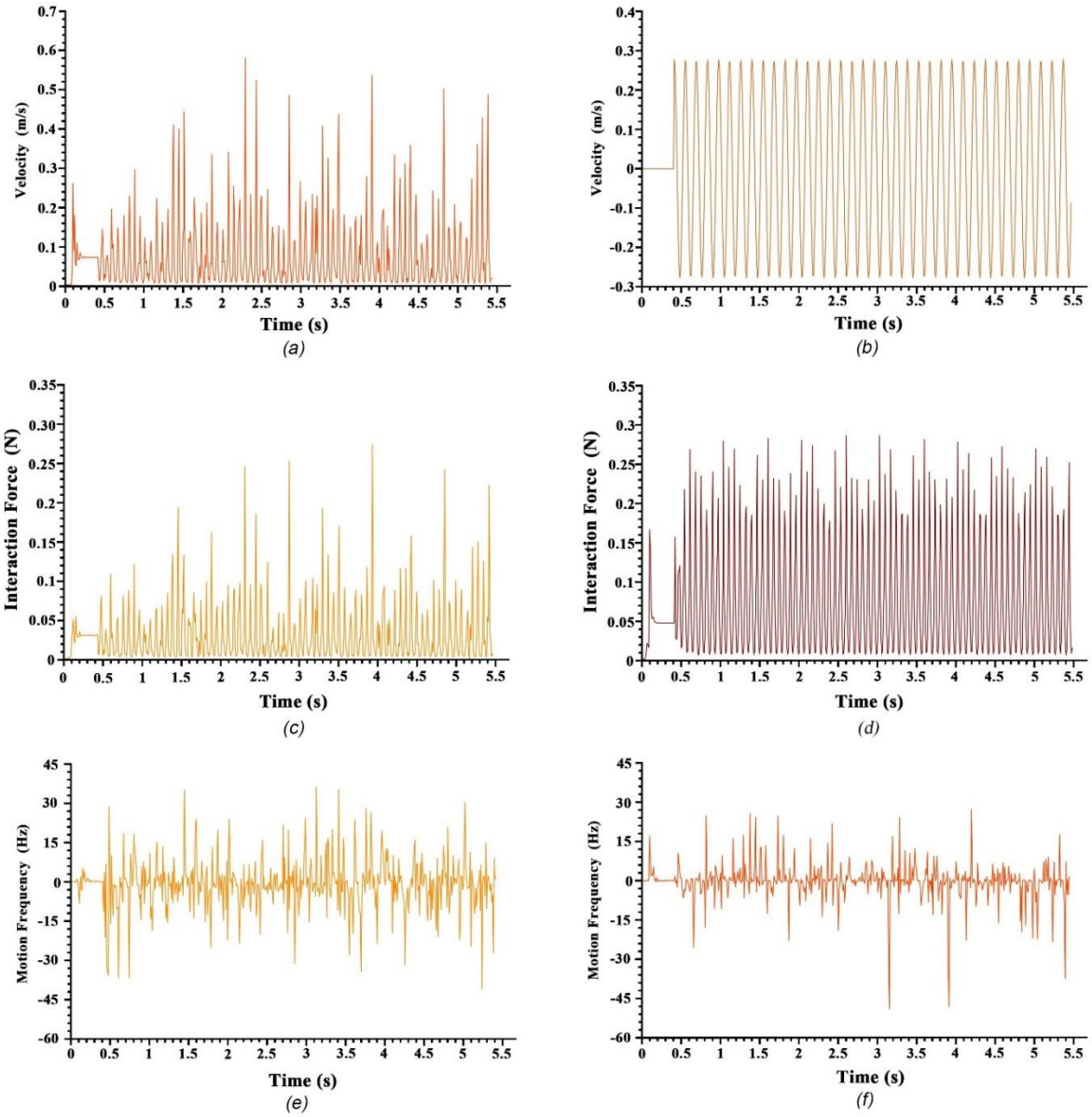

Fig. 12 - Simulation result analysis

(a) Motion speed of tea particles; (b) Kinematic velocity of the pot groove; (c) Interaction force between tea particles; (d) Pot groove interaction force; (e) Movement frequency of tea particles; (f) Movement frequency of pot groove.

RESULTS AND DISCUSSION

Performance test of porous hot air tea de-enzyming and carding machine

To verify the rationality of the designed parameters for the perforated hot-air tea de-enzyming and carding machine, the reliability of its working performance, and whether the quality of finished tea could meet current tea processing quality standards, a machine performance test was carried out in November 2022 in the workshop of Yuanfeng Tea Machinery Co., Ltd., Anji County, Huzhou City, Zhejiang Province. The tea sample used in the test was 'Anji Baiye No.1', and the test instruments and equipment included a stopwatch, an infrared temperature-measuring gun, an electronic platform weighing scale, an electronic balance, and a 6CSL-800 tea de-enzyming and carding machine. These test instruments and prototype are shown in Figure 13 (*Tang et al., 2022*).

Fig. 13 - Test instruments and equipment used

(a) Digital stopwatch; (b) Infrared temperature gun; (c) Electronic platform weighing scale; *(d) Electronic balance; (e) 6CSL-800 tea de-enzyming and carding machine*

Experimental design

The fresh leaves of local white tea cultivated in Anji County were selected as the experimental materials. The motor speed was set to approximately 240 r/min in the process of de-enzyming and 180 r/min for the carding phase; the total time of de-enzyming and carding was 10 min. The withered fresh tea leaves were poured into the pot, the performance of the prototype was tested thrice, and the average value of the three tests groups taken as the final test result. The actual empirical testing site is shown in Figure 14. Because no special test method and operation quality index are yet available for the performance of tea de-enzyming and carding machines in China, this test mainly refers to existing standards and requirements, specifically JB/T 10808—2007 “Tea Processing Equipment”, JB/T 12833—2016 “Tea Carding Machine”, and GB/T 23776—2018 “Tea Sensory Evaluation Method”. The test indices mainly included an output per hour, bar-type rate, de-enzyming suitability rate, pot groove surface temperature, and tea sensory evaluation index *(Zhang K. et al., 2020*).

(1) Output per hour: A stopwatch was used to record the time required for finishing one round of de-enzyming and carding, and the total quantity of tea at the end of the test was weighed. Hourly output is calculated this way:

$$P_1 = \frac{M_1}{t} \tag{17}$$

where: P_1 is the output per hour (kg/h); M_1 is the total mass of tea at the end of the experiment (kg); and t is the time required to complete a de-enzyming and carding (h).

(2) Bar-type rate: Of the processed dry tea, 100 g was taken; any excess impurities, such as broken tea, tea stems, and yellow leaves, were picked out, and the remainder divided into strip leaves and non-strip leaves accordingly. The sum of the two and their respective weights were measured, and then their average after

many experimental runs was taken. The percentage of strip and non-strip leaves in the dry tea samples was calculated by the weighing method, with bar-type rate determined as follows:

$$Y_1 = \frac{Q_1}{T_q} \times 100\% \quad (18)$$

where:

Y_1 is the bar-type rate (%;) Q_1 is the qualified quality of strip leaves (kg;) and T_q is the sum of the quality of strips leaves and the quality of non-strips leaves (kg).

(3) Following the requirements of the JB/T12833-2016 Tea Carding Machine, a prototype test was conducted in which the *de-enzyming suitability rate* served as the final evaluation index. At the end of the de-enzyming process, the dry tea sample was sampled (ca. 300 g). The weight of fresh leaves was measured on an electronic platform scale; the dry weight of fresh leaves per unit of time was calculated; and the red leaves, yellow leaves, burnt leaves, older leaves, and moderate leaves were selected and respectively weighed *(Liu et al., 2023*). The suitable degree of de-enzyming was determined by measuring the morphological characteristics and the content of its inclusions, including the selected de-enzymed moderate leaves for their green color and the sharp seedling-exposed strip-shaped leaves. By measuring the moisture content of fresh leaves of all grades, the de-enzyming suitability rate and the dry weight per unit area under the corresponding moisture content were each calculated. Using those values, the de-enzyming suitability rate was obtained as follows:

$$M_r = \frac{D_q}{M_1} \times 100\% \quad (19)$$

where:

M_r is the de-enzyming suitability rate (%); D_q is the quantity of dry tea that meets the requirements of de-enzyming quality (kg); and M_1 is the total mass of fresh leaves used in the experiment (kg).

(4) *Surface temperature of the pot groove*: The four diagonal positions on the pot groove's surface, the tea outlet, and the radial circumferential direction of the pot groove's inner wall were taken as three measuring points. The temperature of the measuring points within 10–15 cm from the surface of the pot groove was measured using an infrared thermometer. Each point was measured three times, and the average value of the sum of these three temperatures taken as the point temperature. Finally, the average value of the temperatures of the three measured point locations was taken as the effective working temperature of the pot groove.

Fig. 14 - Test site

Testing results

As presented in Table 4, by taking the average of the three machine tests, the hourly output of the test prototype was 3.89 kg/h and the bar-type rate was 89.14%, its de-enzyming suitability rate was 91.67%, with a measured average effective running temperature of the pot groove of 189 °C. Based on these, the performance of the test prototype was assessed and analyzed. As shown in Figure 15, the dry tea samples processed by the experimental prototype were then examined by tea sensory evaluation experts; the resulting evaluation indices met the color requirements for green tea. The sensory evaluation results after three tests are summarized in Table 5.

According to JB/T 10808—2007 Complete “Tea Processing Equipment”, JB/T 12833—2016 “Tea Carding Machine”, and GB/T 23776—2018 “Tea Sensory Evaluation Method”, the quality of the finished tea met the current agronomic standard and satisfied all the performance indices of the 6CSL-800 tea de-enzyming and carding machine. Notably, all the indices were superior to those of the traditional tea de-enzyming and carding machine.

Table 4

Test results

Parameter	First test	Second test	Third test	Mean value
Output per hour (kg·h^{-1})	3.81	3.79	4.08	3.89
Bar-type rate (%)	89.59	86.28	91.65	89.14
De-enzyming appropriate rate (%)	93.73	91.83	89.47	91.67
Surface temperature of the pot groove (°C)	180	210	178	189.3

Table 5

Tea sensory evaluation results

Group	Color	Bar-type	Liquor color	Appraisal result
First test	**Sap green**	**Flat vertical**	**Pale yellow**	**Qualified**
Second test	**Jade green**	**Slightly curved**	**Yellowish**	**Qualified**
Third test	**Green bloom**	**Flat vertical**	**Yellow green**	**Qualified**

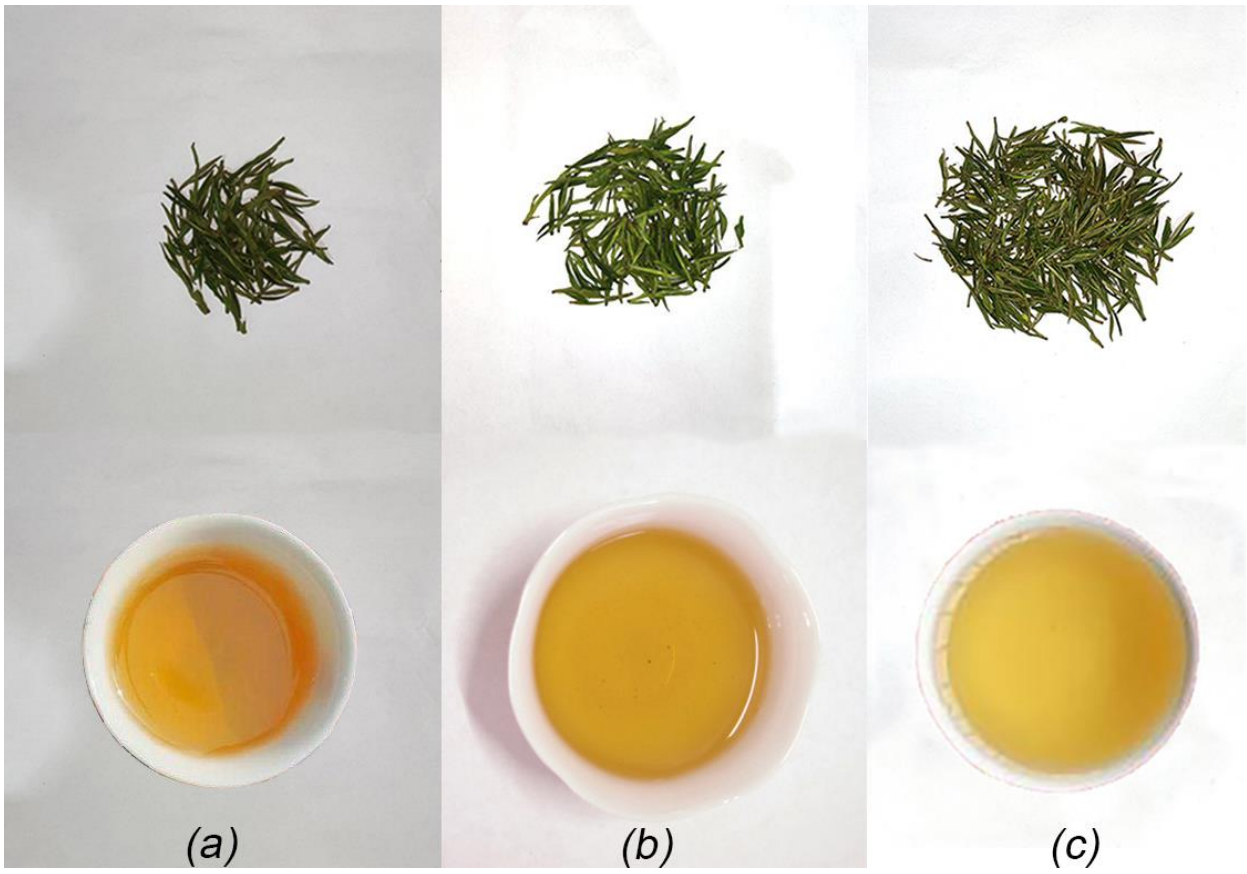

Fig. 15 - Tea evaluation results

(a) The first test; (b) The second test; (c) The third test

CONCLUSIONS

(1) By studying the working process of a porous hot-air tea de-enzyming and carding machine under a gas–solid coupling condition, it was established a mechanical model of tea particles’ movement characteristics through air following the principle of fluid mechanics. Using the coupling simulation method of Rocky-DEM and ANSYS Fluent, continuous and discrete-phase models were established, which verified the feasibility of measuring the movement process of tea in the pot groove on the basis of a gas–solid coupling simulation.

This simulation of tea movement's change process in the pot groove, based on the coupling of gas–solid two-phase flow, demonstrated high accuracy. Hence, it could provide a theoretical reference for the numerical simulation of the same type of tea processing equipment.

(2) The 6CSL-800 tea de-enzyming and carding machine was studied here. Due to numerous, intensive fluid dynamics calculations, a good convergence effect was not attained. Accordingly, the influence of changing the speed of the air inlet upon the coupling effect was not considered. Looking ahead, follow-up experiments could be carried out that alter the air inlet's speed, to further optimize and improve the porous hot air tea de-enzyming and carding machine.

ACKNOWLEDGEMENT

This work was supported by the National Natural Science Foundation of China (52205509), Anhui Provincial Natural Science Foundation Youth Fund Program (2208085QE155), Open Fund Program of State Key Laboratory of Tea Plant Biology and Utilization (SKLTOF20220118), and the Yuanfeng Tea Processing Technology Research and Quality Service Enhancement Enterprise Commissioning Project (KJ2022436).

REFERENCES

[1] Bi, H., Jia, P., Qin, K., Yu, L., Cao, C., and Bai, Y. (2022). Optimization design of pot slot structure of tea de-enzyming and carding machine. *Agronomy* [Basel]. 12: 2937. https://doi.org/10.3390/agronomy12122937.

[2] Cao, C., Wu, Z., Liang, S., and Ge Liangzhi. (2016). Design and experiment of double fuzzy control system for tea cylinder water-removing machine. *Transactions of the Chinese Society for Agricultural Machinery.* 47: 259-65. https://doi.org/11.1964/s.20160512.1031.008.

[3] Geitani El T., Blais, B. (2023). Solid-liquid rotary kilns: An experimental and CFD-DEM study. *Powder Technology*. 430: 119008. https://doi.org/10.1016/j.powtec.2023.119008.

[4] Li, Y., Liu, R., Liu, C., and Liu. L. (2021). Simulation determination and test of seed velocity coupling in the seed delivery tube of air-fed seed dispenser. *Transactions of the Chinese Society for Agricultural Machinery.* 52: 54-61+133.

[5] Liu, S., Cao, C., Ge, J., Zhao, C., Wu, Z., and Sun, Y. (2023). Design and simulation of a hot air drum killing machine with thermal energy circulation. *Journal of Agricultural Mechanization Research.* 45: 107-114. https://doi.org/10.13427/j.cnki.njyi.2023.10.032.

[6] Luo, K., Cao, C., Wu, Z., Zhang, X., and An, M. (2022). Optimization of roasted green tea winnowing via fluid–solid interaction experiments and simulations. *Foods.* 11: 3271. doi: 10.3390/foods11203271.

[7] Luo, K., Wu, Z., Cao, C., Qin, K., Zhang, X., An, M. (2022). Biomechanical characterization of bionic mechanical harvesting of tea buds. *Agriculture*. 12: 1361. https://doi.org/10.3390/agriculture12091361.

[8] Luo, K., Wu, Z., Cao, C., Qin, K., Zhang, X., and Zhong, H. (2022). Design and experiment of a combined pinch-and-cut picker for fresh tea leaves. *Transactions of the Chinese Society of Agricultural Engineering.* 38: 1-9.

[9] Michiko, S., Akiko, M., Stephen, H., Yasufumi, S., Naoki, F., Emiko, S., Kanae, A., Koichi M, I. (2017). EDEM Function in ERAD Protects against Chronic ER Proteinopathy and Age-Related Physiological Decline in Drosophila. *Developmental Cell.* 41: 652-664. https://doi.org/10.1016/j.devcel.2017.05.019.

[10] Panchariya, P., Popovic, D., Sharma, A. (2002). Thin-layer modelling of black tea drying process. *Journal of Food Engineering*. 52: 349-357. https://doi.org/10.1016/S0260-8774(01)00126-1.

[11] Qin, K., Zhang, Y., Shen, Z., Cao, C., Wu, Z., Ge, J., Fang, L., and Bi, H. (2022). Investigating the coupling effect of high pressure and hot air on external friction angle based on resistance reduction tests on subsoiling tillage tools for sandy clay loam. *Agronomy [Basel].* 12: 2663. https://doi.org/ 10.3390/agronomy12112663.

[12] Qin, K., Zhao, Y., Zhang, Y., Cao, C., and Shen, Z. (2022). Lateral stress and its transmission law caused by operation of a double-wing subsoiler in sandy loam soil. *Frontiers in Environmental Science.* 1873. https://doi.org/10.3389/fenvs.2022.986361.

[13] Rakesh, K., Shibayan, S. (2023). Erosion analysis of radial flow hydraulic turbine components through FLUENT-EDEM coupling. *Powder Technology*. 428: 118800. https://doi.org/10.1016/j.powtec.2023.118800.

[14] Shi, C., Zhang, X., Zhong, J., Qiao, X., Dai, H. (2015). Research on hot air killing process and structure optimization of killing machine based on multiphase flow coupling. *Journal of Mechanical & Electrical Engineering*. 32: 1050-1055.

[15] Tang, H., Xu, C., Qi, X., Wang, Z., Wang, J., Zhou, W., Wang, Q., and Wang, J. (2021). Study on periodic pulsation characteristics of corn grain in a grain cylinder during the unloading stage. *Foods.* 10: 2314. https://doi.org/10.3390/foods10102314.

[16] Tang, H., Xu, C., Xu, W., Xu, Y., Xiang, Y., and Wang, J. (2022). Method of straw ditch-buried returning, development of supporting machine and analysis of influencing factors. *Frontiers in Plant Science.* 13: 967838. https://doi.org/10.3389/fpls.2022.967838.

[17] Tang, H., Xu, C., Wang, Z., Wang, Q., and Wang, J. (2022). Optimized design, monitoring system development and experiment for a long-belt finger-clip precision corn seed metering device. *Frontiers in Plant Science.*13: 814747. https://doi.org/10.3389/fpls.2022.814747.

[18] Wang, P., Yi, W., Cheng, F., Wang, C., Zhou, Y., Deng, J. (2022). CFD-based experiments and optimization of tea baring components. *Journal of Chinese Agricultural Mechanization*. 43: 86-91. https://doi.org/10.13733/j.jcam.issn.2095-5553.2022.10.013.

[19] Wang, X., Wu, Z., Zhong, H., Huang, Y., Zhang, X., and Shi Z. (2022). Evaluation of the tea carding operation based on machine vision technology. *China Tea Processing.* 3: 40-45. https://doi.org/10.15905/j.cnki.33-1157/ts.2022.03.001.

[20] Wu, Z., Cao, C., Wang, E., Luo, K., Zhang, J., and Sun, Y. (2019). A method for tea selection based on morphological feature parameters. *Transactions of the Chinese Society for Agricultural Machinery.* 35: 315-21.

[21] Wu, Z., Huang, Y., Ouyang, T., Luo, K., Qin, K., Sun, Y. and Cao, C. (2022). Design and test of precise regulation system for process parameters of double-layer tea winnowing machine. *Agriculture.* 12: 1584. https://doi.org/10.3390/agriculture12101584.

[22] Wu, Z., Luo, K., Cao, C., Liu, G., Wang, E., and Li, W., (2020). Fast location and classification of small targets using region segmentation and a convolutional neural network. *Computers and Electronics in Agriculture.* 169: 105207. https://doi.org/10.1016/j.compag.2019.105207.

[23] Xu, H., Tan, H., Li, G., Xie, Chi., Li, J. (2014). Study on the spiral motion model of leaf guide plate of roller type tea killing machine. *Journal of Tea Science*. 34: 381-386. https://doi.org/10.13305/j.cnki.jts.2014.04.009.

[24] Xue, K., Gao, K., Kuang, F., Zhang, S., Liao, J., and Zhu, D. (2022). Machinery-plant-paddy soil coupling model based numerical simulation method of mechanical transplanting process of big rice seedling. *Computers and Electronics in Agriculture.* 198: 107053. https://doi.org/10.1016/j.compag.2022.107053.

[25] Ye, F., Gao, S., Gong, Z., Zhang, Q., Teng, J., Hou, W., Liang, B. (2014). Effect of different killing methods on the quality of green tea. *Journal of Sichuan Agricultural University*. 32: 160-164+171.

[26] Yan, J., Hu, D., Liu, Q., Yu, L., and Niu, S. (2022). Research progress of tea leaf striping technology and machinery. *Journal of Chinese Agricultural Mechanization.* 43: 75-83. https://doi.org/10.13733/j.jcam.issn.2095-5553.2022.02.011.

[27] You, Q., Shi, Y., Zhu, Y., Yang, G., Yan, H., Lin, Z., and Lv, H. (2023). Influence of different manufacturing processes on the key aroma-active compounds of green tea. *Food Science*. 1-14. https://doi.org/ 11.2206/TS.20221110.2102.022.

[28] Yu, W., Wu, R., Li, H., Pei, G., Jin, S., Huang, C., Zhu, R., Yang, P., Xiong, H. (2019). Numerical simulation of flow field inside the drum of tea infrared killing machine based on Fluent-EDEM coupling. *Food & Machinery*. 35: 104-109+120. https://doi.org/10.13652/j.issn.1003-5788.2019.08.020.

[29] Zhang, K., Wang, W., Zhao, X., and Liu, X. (2020). Design and test of a roller-type tea hot air re-drying machine. *Transactions of the Chinese Society for Agricultural Machinery.* 51: 377-86.

[30] Zhang, S., Tekeste, M., Li, Y., Gaul, A., Zhu, D., and Liao, J. (2020). Scaled-up rice grain modelling for DEM calibration and the validation of hopper flow. *Biosystems Engineering.* 194: 196-212. https://doi.org/ 10.1016/j.biosystemseng.2020.03.018.

[31] Zhang, Y., Tian, L., Cao, C., Zhu, C., Qin, K., and Ge, J. (2022). Optimization and validation of blade parameters for inter-row weeding wheel in paddy fields. *Frontiers in Plant Science.* 13: 1003471. https://doi.org/10.3389/fpls.2022.1003471.